

Direct signal recovery from threshold crossings

May Lim and Caesar Saloma*

National Institute of Physics, University of the Philippines, Diliman 1101, Quezon City, Philippines

(Received 12 September 1997; revised manuscript received 4 May 1998)

We present a method for directly obtaining the $2M$ equally sampled amplitude values of the analog input signal $s(t)$ from the $2M$ locations $\{t_i\}$ where it intersects with a reference signal $r(t) = A \cos(2\pi f_r t)$. Until now, high-accuracy signal recovery in sinusoid-crossing sampling had been achieved only indirectly using spectral methods. The recovery requirements are (1) $|s(t)| < A$ and (2) $W \leq 2f_r$, where W is the bandwidth of $s(t)$. The recovery method is evaluated as a function of the accuracy in which the crossings are located, and the sampling period $T = 2M\Delta$, where $\Delta = 1/2f_r$. Its performance is also compared with other direct interpolation schemes. [S1063-651X(98)11610-0]

PACS number(s): 07.05.Kf, 02.60.Gf

I. INTRODUCTION

Previous schemes for accurately recovering a band-limited signal $s(t)$ from its sinusoid-crossing (SC) locations $\{t_i\}$ have been done only indirectly using spectral methods [1,2]. The Fourier components $\{c(m)\}$ are first calculated directly from $\{t_i\}$ where $i = 1, 2, \dots, 2M$, and $m = -M, -M+1, \dots, M$. Equally sampled amplitude values $\{s(k)\}$ of $s(t)$ are then recovered by inverse Fourier transforming $\{c(m)\}$, where $k = (2i-1)(\Delta/2)$ is the midpoint of the i th sampling interval Δ_i .

Threshold sampling is attractive because it can be implemented with a single-comparator circuit, which in essence is simply a one-bit analog-to-digital (AD) converter with only two (2^1) possible output states—the high and low states [3]. The main challenge in threshold sampling is in recovering the correct analytic values of $s(t)$ from the locations $\{t_i\}$ of its intersections with the reference signal $r(t)$.

This paper demonstrates a method for calculating $\{s(k)\}$ directly from $\{t_i\}$. This capability is important in signal processing because many integral and differential equations are solved numerically using equally sampled sets of data values [4]. The recovery method is suitable to signals with no meaningful Fourier transforms (e.g., noise and stochastic signals [5]) where the spectral-based method is inapplicable.

Direct signal recovery is also relevant in our quest to understand the nature of information coding and decoding in biological systems which can utilize threshold sampling to encode an external stimulus. The time variations in the input stimulus value are encoded either as changes in the neuronal firing rate (amplitude-to-frequency conversion) or as variations in the delay time that an action potential generates with respect to some reference time (temporal coding) [6–11]. In both coding schemes, there has been no clear experimental evidence that the threshold representation must first pass through Fourier domain decomposition before an amplitude representation of the input stimulus is generated.

Hopfield [8] has used a sinusoid reference signal to model the delay in the firing of an action potential in response to a particular input stimulus value (phase coding). Experimental evidence has been found regarding the existence of such oscillatory reference patterns in the hippocampal place cells in rats [12] and electric fish [13].

The ability to recover accurately the $s(t)$ value at any time t within the sampling period T , from its data representation of unequally sampled $s(t)$ values, is also important in geology, population biology, and ecosystem science (e.g., in earthquake monitoring [14], and population and disease coding [15]), where amplitude measurements at equal time intervals are difficult to implement. Although other direct interpolation schemes, such as polynomial curve-fitting and cubic-spline interpolation, may also be applied to approximate $\{s(k)\}$ from $\{r(t_i)\}$, the results may be highly inaccurate depending on the behavior of $s(t)$.

II. THEORY

A. Sinusoid-crossing sampling

The SC locations $\{t_i\}$ are solutions to $s(t) - r(t) = 0$, where $r(t) = A \cos(2\pi f_r t)$. The set $\{t_i\}$ contains complete information about $s(t)$ provided that it is obtained using [16]: (1) $A > |s(t)|$ for all t values, and (2) $f_r \geq W/2$, which is the highest frequency of $s(t)$. In such conditions, an SC exists within each interval $\Delta = 1/(2f_r)$, and SC sampling satisfies the Nyquist sampling criterion for band-limited continuous-time signals with highest frequency $W/2$ (signal bandwidth is denoted by W).

We have previously shown that the Fourier spectrum of $s(t)$ can be derived accurately from $\{t_i\}$ for the practical case where the number $2M$ of t_i is large [2]. When $2M$ is large ($2M > 32$), the composite signal $[s(t) - r(t)]$ cannot be reconstructed simply as a product series of its $2M$ roots, because of the ill effects of the rounding-off errors [17]. Equally sampled amplitude values $\{s(k)\}$ of $s(t)$ may be obtained by inverse transforming the Fourier spectrum, where $k = (2i-1)\Delta/2$ [1].

In this work, we show a method for accurately deriving $\{s(k)\}$ directly from $\{t_i\}$ without the need to calculate first for the Fourier spectrum. It makes use of the Nyquist sampling theorem and the ideal interpolation formula [18,19].

*Author to whom correspondence should be addressed. FAX: +632-920 5474. Electronic address: csaloma@nip.upd.edu.ph

From $\{t_i\}$ one can obtain a set of nonuniformly sampled amplitude representation of $s(t)$ given by $\{s(t_i)\} = \{r(t_i)\}$. The $\{r(t_i)\}$ contains one sampled value of $s(t)$ within each Δ , because an SC exists within each Δ of the sampling period $T = 2M\Delta$.

B. The ideal interpolation formula

The Nyquist sampling theorem states that [18,19] any band-limited continuous function $s(t)$ with highest frequency $W/2$, can be uniquely recovered from $\{s(k)\}$ if it is obtained using a sampling interval $\Delta \leq 1/W$.

The recovery is achieved using the ideal interpolation formula [19], which permits the calculation of the amplitude of $s(t)$ at any arbitrary time t (within T), from $\{s(k)\}$:

$$s(t) = \Delta \sum_{n=-\infty}^{\infty} s\left(\frac{(2n-1)\Delta}{2}\right) \frac{\sin\{2\pi f_c[t - (2n-1)\Delta/2]\}}{\pi[t - (2n-1)\Delta/2]}. \quad (1)$$

Equation (1) yields an exact solution for $s(t)$ if and only if (1) an infinite number of $s(k)$ terms are used in the expansion, and (2) no quantization errors are found in $\{s(k)\}$.

For our case, we have a data set $\{s(t_i)\} = \{r(t_i)\}$, representing known values of $s(t)$ at locations $\{t_i\}$ where $s(t) = r(t)$. The $\{r(t_i)\}$ contains a representative value of $s(t)$ in each of the Δ 's of the sampling period, which implies that $\{r(t_i)\}$ contains complete information about $s(t)$ that could be used to solve for $\{s(k)\}$.

The inverse problem of solving for $\{s(k)\}$ from $\{r(t_i)\}$ via Eq. (1) is well posed because the number of unknowns and input data points are equal—for every unknown $s(k)$ value in a given interval Δ_i , there is a corresponding known value of $s(t_i) = r(t_i)$. Equation (1) is then expressed as

$$r(t_i) = \Delta \sum_{n=-\infty}^{\infty} s\left(\frac{(2n-1)\Delta}{2}\right) \frac{\sin\{2\pi f_c[t_i - (2n-1)\Delta/2]\}}{\pi[t_i - (2n-1)\Delta/2]}. \quad (2a)$$

Equation (2a) yields the exact solutions for all the elements in $\{s(k)\}$ if and only if $\{r(t_i)\}$ has an infinite number of elements, and does not have quantization errors.

Let $\{t'_i\}$, $\{t''_i\}$, and $\{t_i\}$ be the respective SC's [with respect to a common $r(t)$] of the band-limited signals $s_1(t)$, $s_2(t)$, and $s(t)$. Equation (2a) can be used to obtain the following equally sampled representations: $\{s_1(k)\}$, $\{s_2(k)\}$, and $\{s(k)\}$ from $\{r(t'_i)\}$, $\{r(t''_i)\}$, and $\{r(t_i)\}$, respectively.

If $s(t) = s_1(t) + s_2(t)$, then $s(k) = s_1(k) + s_2(k)$. Thus the same $\{s(k)\}$ is obtained from Eq. (2a) using $\{r(t_i)\}$, or as a sum of $\{s_1(k)\}$ and $\{s_2(k)\}$. This property strictly holds only if $\{r(t'_i)\}$, $\{r(t''_i)\}$, and $\{r(t_i)\}$ all have infinite elements and are not affected by quantization errors.

In practice, only a finite number $2M$ of SC's is obtained and the convolution process in Eq. (2a) is truncated to

$$r(t_i) = \Delta \sum_{n=1}^{2M} s\left(\frac{(2n-1)\Delta}{2}\right) \frac{\sin\{2\pi f_c[t_i - (2n-1)\Delta/2]\}}{\pi[t_i - (2n-1)\Delta/2]}. \quad (2b)$$

Equation (2b) provides a set of $2M$ equations in $2M$ unknowns. Solving for the $2M$ unknowns using the LU De-

composition technique [20] would involve $(1/3)(2M)^3 + (2M)^2$ computational operations.

Furthermore, the SC's can be located only with finite accuracy, which leads to quantization errors in our representation of $\{s(t_i)\}$ by $\{r(t_i)\}$ [1–3]. In this paper, we investigate numerically how the quantization errors and the use of a finite $2M$ value, affects the accuracy of the calculated $s(k)$ values.

It has been shown recently that when $2M$ is finite, the exact sinc interpolation in Eq. (1) may be replaced by [21,22]

$$r(t_i) = \sum_{n=1}^{2M} s\left(\frac{(2n-1)\Delta}{2}\right) \frac{\sin\left\{2\pi f_c\left[t_i - \frac{(2n-1)\Delta}{2}\right]\right\}}{2M \sin\left\{\frac{1}{2M} 2\pi f_c\left[t_i - \frac{(2n-1)\Delta}{2}\right]\right\}}. \quad (3)$$

We also examine the difference between using Eq. (2b) and Eq. (3), in solving for the unknown $s(k)$ values.

C. Quantization errors in sinusoid crossing sampling

An SC is located by subdividing each Δ into N partitions of size $\delta = \Delta/N$, so that $T = 2MN\delta$ [1–3]. The SC location in the i th interval Δ_i is given by $t_i = (i-1)N\delta + p_i\delta$, where p_i is the partition location [$0 \leq p_i \leq (N-1)$] within Δ_i where $s(t) = r(t)$.

In a real SC detector [3], the smallest possible δ value is given by the response time, which is always finite. In numerical experiments, the δ value is also finite because Δ cannot be subdivided into an infinite number of partitions. Thus, an uncertainty exists in the measured location of the intersection between $s(t)$ and $r(t)$ within the i th interval Δ_i . This uncertainty gives rise to a quantization error $E(t_i)$ in our representation of $s(t_i)$ by $r(t_i)$ [3].

In the first-order approximation, the measured value of $s(t_i)$ is represented by $r(t_i)$, according to $s(t_i) = r(t_i) \pm E(t_i)$, where $E(t_i) = (1/2)|[\partial r(t)/\partial t]dt|$, evaluated at $t = t_i$. By noting that $dt = \delta$, $f_r = 1/2\Delta = 1/2N\delta$, we obtain $E(t_i) = (A\pi/2N)|\sin(\pi t_i/N\delta)|$, where $t_i = (i-1)N\delta + p_i\delta$. Note that $E(t_i)$ becomes infinitely small when N is made infinitely large.

The largest possible value for the error is $E_{\max} = A\pi/2N$, which occurs at t_i locations where $r(t) = 0$. Thus, $r(t_i)$'s representing $s(t)$ values that are near zero are the most inaccurate. On the other hand, $r(t_i)$'s representing $s(t)$ values that are near the reference amplitude A are least affected by quantization errors.

For given values of the SC sampling parameters (A , N , T , f_r , and δ), the $E(t_i)$ value varies from one interval Δ to another according to how the $s(t)$ value changes within these sampling intervals. For example, the $\{r(t_i)\}$ representing the dc signal $s(t) = A$, contain the least amount of quantization errors because all the SC's occur at locations where $r(t) = A$. On the other hand, the $\{r(t_i)\}$ representing the dc signal $s(t) = 0$, is the most inaccurate because the SC's occur at locations where $r(t) = 0$. If $s(t)$ is a sinusoid of frequency

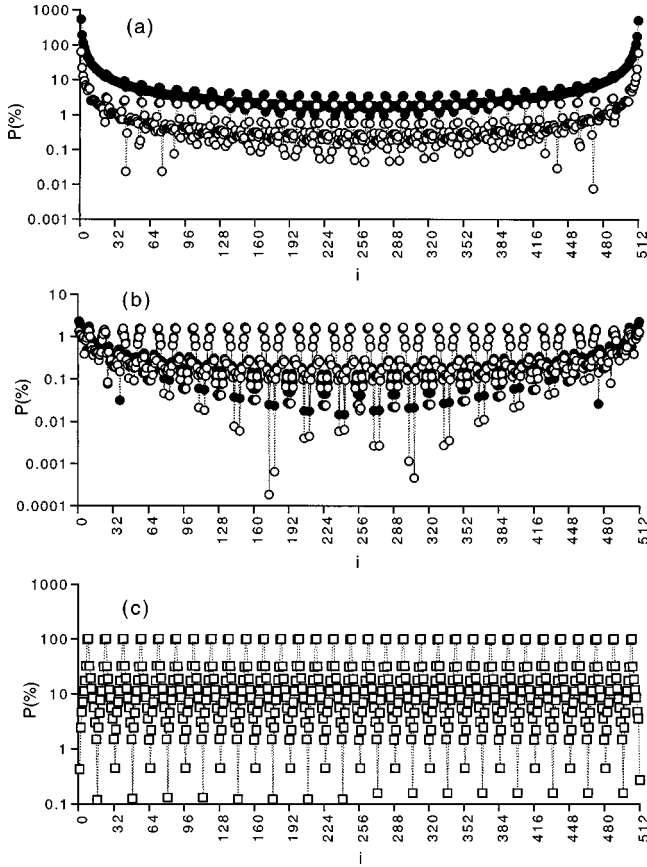


FIG. 1. Percentage error P vs i plots when $\{s(k)\}$ is recovered using Eq. (2b) (open circles) and Eq. (3) (closed circles) for (a) $T = 2M\Delta$, (b) extended $T = (2M + 10)\Delta$, and (c) cubic spline interpolation (squares) with $T = 2M\Delta$. Parameters used are $k = (2i - 1)(\Delta/2)$, $s(t) = 1.0 \cos(2\pi 16t)$, $r(t) = 2.5 \cos(2\pi 256t)$, $\Delta = 1/512$, $2M = 512$, and $N = 1000$.

f_s , we expect the ill effects of the quantization errors to exhibit the periodicity of f_s .

III. NUMERICAL EXPERIMENTS

A. Sinusoid test signals

We first evaluate the performance of our interpolation technique to sinusoid input signals of the form $s(t) = A_s \cos(2\pi f_s t + \varphi)$. Numerous values are considered for the frequency f_s , amplitude A_s , and phase φ . Sinusoids are suitable test signals because any band-limited periodic function can be expressed as a linear superposition of weighted sinusoids of appropriate frequencies and phases. They also permit an easy analysis of the effects of quantization errors on $\{s(k)\}$.

Figure 1(a) plots the percentage error $P(k) = 100|s_i(k) - s_c(k)|/s_i(k)$, where $\{s_i(k)\}$ and $\{s_c(k)\}$ represent the true and calculated equally sampled values of $s(t)$, respectively. The $P(k)$ plots compare the accuracy of $\{s_c(k)\}$ when it is obtained using Eq. (2b) (open circles), and Eq. (3) (closed circles) for $s(t) = 2.45 \cos(2\pi 16t)$, $r(t) = 2.5 \cos(2\pi 256t)$, $T = 1$, $2M = 512$, $N = 1000$, and $\delta = T/2MN = 1.953 \times 10^{-6}$ [23]. The SC's are located at an accuracy of 1 in 1000 within each Δ .

The largest quantization error possible is $E_{\max} = A\pi/2N \approx 0.004$, and they occur in the corresponding $r(t_i)$ represen-

tations of $s(t)$ values that are equal and near to zero. Percentage errors are at their minimum at t_i locations where $s(t_i) = A_s \approx A$. Although $E(t_i) = E_{\min} \approx 0$, at all these positions, their corresponding $P(k)$ values are not. The accuracy of the computed $s(k)$ value in Δ_i is affected primarily by the quantization error found in its corresponding $r(t_i)$ value, but it is also affected partly by the errors that are incurred in the neighboring sampling intervals.

The $P(k)$ values (circles) produced by Eq. (2b) are about an order of magnitude less than the ones (solid circles) produced by Eq. (3). As predicted in our error analysis, the $P(k)$ plots exhibit the periodicity of $s(t)$ —the P values are largest (at about 10%) at $t = k/512$, for $k = 8, 24, 36, \dots$, where $s(t) = 0$.

The P values are exceptionally large ($>10\%$) at the edges of the data series due to truncation errors that happen when a convolution integral is implemented with only a finite number of data points. To minimize the unwanted ringings at the two edges of $\{s_c(k)\}$, we sampled $s(t)$ using an extended sampling period of $T = (2M + \kappa)\Delta$, instead of just $T = 2M\Delta$, where κ is an even number that is chosen (1) to reduce both $P(k=0)$ and $P(k=511)$ to less than 10%, and (2) to set $P(k=0) \approx P(k=8) \approx \dots \approx P(k=511)$.

We found that $\kappa = 10$ is the least number of additional data points that could satisfy our criterion for at least Eq. (2b) or Eq. (3). The extended sequence $\{r(t_i)\}$ with $(2M + 10)$ elements is utilized to solve for the $(2M + 10)$ unknown $s(k)$ values. The $2M$ $s(k)$ values that are used for comparison are then obtained by truncating $\{s_c(k)\}$ —five points on each side. Figure 1(b) illustrates that the technique is effective in reducing the large errors appearing at the edge of the $s_c(k)$ sequence. The technique has also made the P values produced by Eq. (2b) (open circles) and Eq. (3) (closed circles) comparable with each other. It has also reduced the $P(k)$ values especially in the middle region of the $s_c(k)$ sequence.

Figure 1(c) shows the $P(k)$ plot for $\{s_c(k)\}$ when it is obtained from $\{r(t_i)\}$ using the cubic-spline (CS) interpolation (squares), which is one of the most widely used interpolation methods [20]. The CS interpolation is fast (complexity of order $2M$) and guarantees the global smoothness in the interpolation function up to the first derivative and continuity up to the second derivative. Its corresponding $P(k)$ plot, however, indicates that it is far inferior to the interpolation methods based on either Eq. (2b) or (3). It is not able to yield sufficiently accurate $s_c(k)$ values from $\{r(t_i)\}$.

We now examine the performance of the interpolation procedure as a function of frequency f_s , phase φ , and amplitude A_s . Figure 2 shows the normalized mean-squared error ε versus f_s plots produced by the four recovery techniques that we have been considering. The parameters used are $s(t) = 1.0 \cos(2\pi f_s t)$, $r(t) = 2.5 \cos(2\pi 256t)$, $2M\Delta = 1$, $2M = 512$, $N = 1000$, and $\kappa = 10$. The normalized mean-squared error ε is defined as $\varepsilon = \sum_k [s_c(k) - s_i(k)]^2 / \sum_k s_i^2(k)$.

The CS interpolation (open squares) yielded a $\{s_c(k)\}$ with an ε that increases very rapidly with the f_s value. The behavior of the ε plot that it produced is worse than the one generated using the ‘‘sample-and-hold’’ (SH) method (closed squares), where the $\{s_c(k)\}$ is derived by simply using the approximation $\{s_c(k)\} \cong \{r(t_i)\}$.

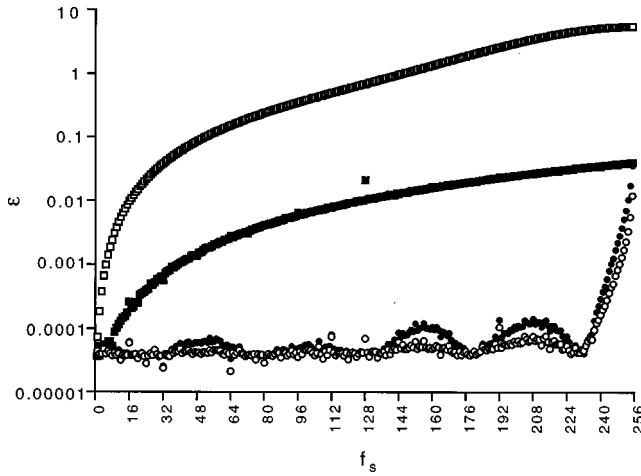


FIG. 2. Normalized mean-squared error ε vs f_s plot using Eq. (2b) (circles), Eq. (3) (closed circles), cubic spline interpolation (squares), sample-and-hold (closed squares) for $s(t) = 1.0 \cos(2\pi f_s t)$, where $r(t) = 2.5 \cos(2\pi 256t)$, $2M = 512$, $\kappa = 10$, and $N = 1000$.

The $\{s_c(k)\}$ produced by either Eq. (2b) (open circles) or Eq. (3) (closed circles) exhibits a significantly lower ε value that is also quite insensitive to f_s within in the range $0 \leq f_s \leq 232 = 0.9f_r$. The ε plots correspond to $\{s(k)\}$'s that are obtained using the extended- T approach ($\kappa = 10$). The final sequence $\{s_c(k)\}$ used to compute a particular ε is obtained by dropping 5 points on each end of the calculated 522-element $s_c(k)$ sequence.

The ε values produced by both Eqs. (2b) and (3), increase abruptly when the f_s value approaches $f_s = 256 = f_r$. At $f_s = 256$, the two plots yield ε values that are of the same order of magnitude as that shown by the SH plot.

Figure 3 shows the ε versus phase φ (in degrees) plots for the case of $s(t) = 1.0 \cos(2\pi 16t + \varphi)$, $r(t) = 2.5 \cos(2\pi 256t)$, $\kappa = 10$, $2M = 512$, and $N = 1000$. All plots show that the ε value has no phase dependence. Results also

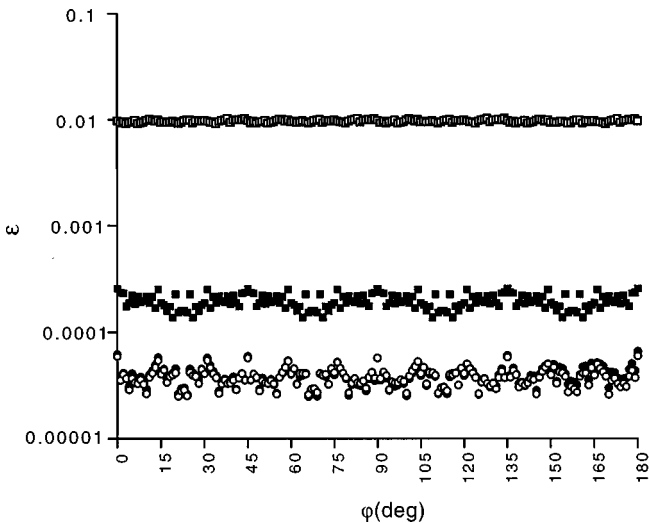


FIG. 3. Normalized mean-squared error ε vs phase φ plot using Eq. (2b) (open circles), Eq. (3) (closed circles), cubic spline interpolation (squares), sample-and-hold (closed squares) for $s(t) = 1.0 \cos(2\pi 16t + \varphi)$, where $r(t) = 2.5 \cos(2\pi 256t)$, $\Delta = 1/512$, $2M = 512$, $\kappa = 10$, and $N = 1000$.

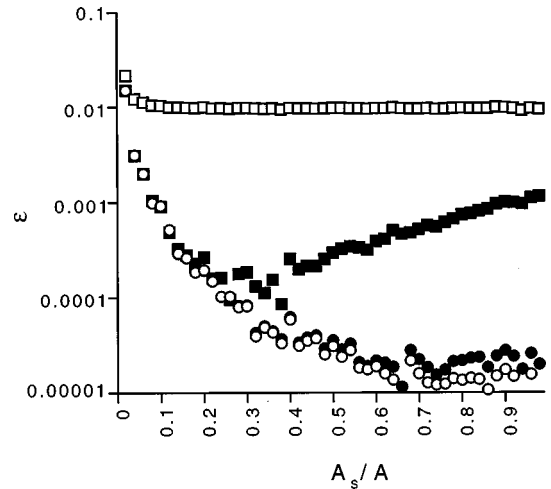


FIG. 4. Normalized mean-squared error ε vs (A_s/A) plots using Eq. (2b) (circles), Eq. (3) (closed circles), cubic spline interpolation (squares), sample-and-hold (closed squares) for the case of $s(t) = A_s \cos(2\pi 16t)$, where $r(t) = A \cos(2\pi 256t)$, $A = 2.5$, $\Delta = 1/512$, $2M = 512$, $\kappa = 10$, and $N = 1000$.

show that Eq. (2b) (open circles) and Eq. (3) (closed circles) produce better results than the CS (squares) and the SH (closed squares) methods. Figures 2 and 3 illustrate that the ε produced by the extended versions of either Eqs. (2b) and (3) does not vary significantly with f_s and φ respectively, at least for $0 < f_s < 0.9f_r$ and $0 < \varphi < \pi$.

Figure 4 shows the ε vs (A_s/A) plots for the case of $s(t) = A_s \cos(2\pi 16t)$, $r(t) = A \cos(2\pi 256t)$, $A = 2.5$, $\kappa = 10$, $2M = 512$, and $N = 1000$. In all the interpolation methods, the ε value is always highest at A_s/A values near zero where the denominators [representing the true $s(t)$ values] in the corresponding ε expressions take on very small values.

The recovery performance of both Eq. (2b) (open circles) and Eq. (3) (closed circles) improves as A_s approaches A , where the number of SC's (out of $2M = 512$) that occur at locations closer to where $r(t) = A$ also increases. At these SC locations, the quantization errors are smaller.

The performance of CS interpolation (squares) is not as good and does not vary very much with the (A_s/A) value. On the other hand, the SH method (closed squares) is best at $A_s/A \approx 0.3$. It exhibits a performance that deteriorates exponentially with (A_s/A) for $(A_s/A) > 0.3$.

In a real SC detector [3], the smallest possible size for δ cannot be smaller than the effective circuit response δ_c . There is an invariant quantity $\delta_c = T/2MN$, which leads to a tradeoff between the accuracy in which we can locate an SC within $\Delta = N\delta = T/2M$, and the value of the cutoff frequency $f_r = M/T$.

For a fixed T , the use of a faster f_r (done by increasing M) necessarily reduces the possible number N of partitions that can be fitted within Δ . On the other hand, increasing N to improve the location accuracy necessarily reduces the $2M$ value. We investigate whether an optimal combination exists between the values of N and M for given values of T and δ .

B. Multifrequency signal

Figure 5(a) plots the ε versus u plots obtained for the band-limited ($W/2 \approx 16$) signal $s(t) = \cos^{200}(2t - 0.25)$

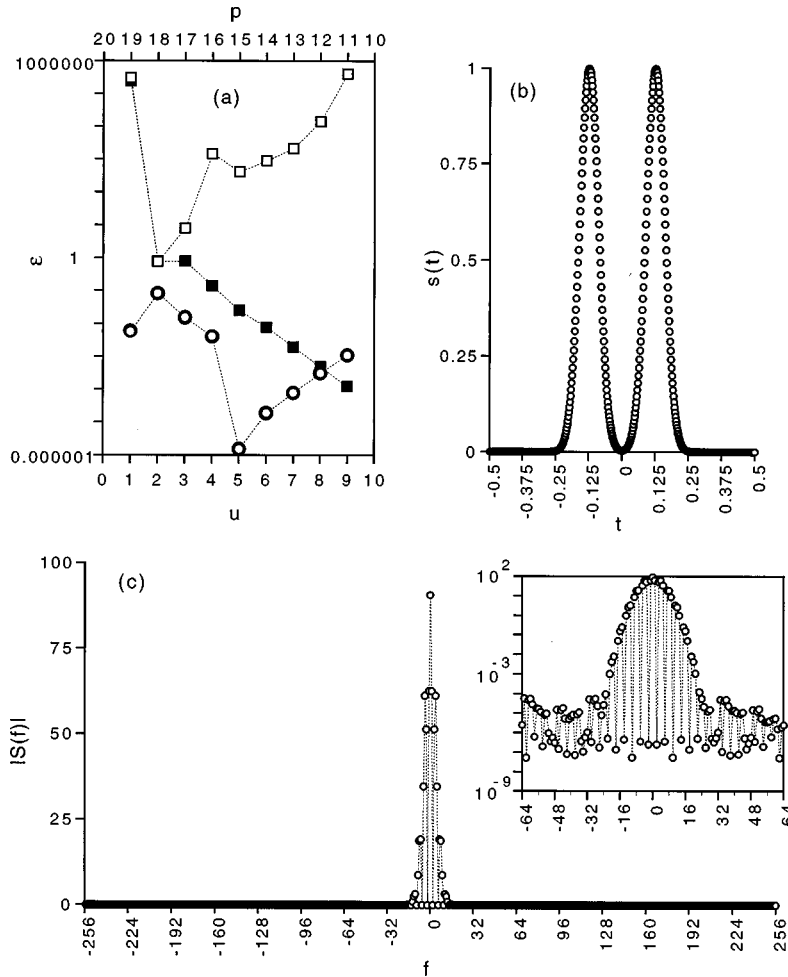


FIG. 5. (a) Normalized mean-squared error ε vs q plots using Eq. (2b) (open circles), Eq. (3) (closed circles), cubic spline interpolation (squares), sample-and-hold (closed squares) where $2M=2^u$, $N=2^p$, $T=2MN\delta=1$, $\delta=2^{-20}$, $s(t)=\cos^{200}(2t-0.25)+\cos^{200}(2t+0.25)$, and $r(t)=2.5\cos(2\pi Mt)$, (b) $s(t)$ vs t plot, and (c) modulus spectrum $|S(f)|$ of $s(t)$. The ε is minimum near $2M=2^5$ or $N=2^{15}$. The results produced by Eqs. (2b) and (3) are essentially identical (circles and closed circles superimposed on each other).

$+\cos^{200}(2t+0.25)$, where $2M=2^u$, $N=2^p$, $2MN\delta=1$, $\delta=2^{-20}$, $\kappa=10$, $f_r=1/2\Delta$, and $r(t)=2.5\cos(2\pi f_r t)=2.5\cos(2\pi Mt)$. The function $s(t)$ is illustrated in Fig. 5(b). Its corresponding modulus Fourier spectrum $|S(f)|$ is shown in Fig. 5(c). The inset plot shows an expanded version of $|S(f)|$.

The ε plots corresponding to Eq. (2b) (open circles) and Eq. (3) (closed circles), exhibit a minimum value of around 10^{-6} , at $u=5$, which is the case when $s(t)$ is sampled using $f_r=M/T=2^4=W/2(N=2^{15})$. The SC's are located with an accuracy of 1 in $2^{15}=32\,768$, within each interval Δ .

The interpolation method yields accurate results for a multifrequency signal particularly if the SC sampling is done with $f_r=W/2$. *A priori* knowledge of the bandwidth of $s(t)$, therefore, is an important piece of information that can be utilized to optimize the performance of the method.

For values of $2M>2^5$, the ill effects of quantization errors dominate in the interpolation procedure and ε increases rapidly with increasing $2M$ value. For $2M<2^5$, $s(t)$ is undersampled and the effect of aliasing is the main contributor to the ε increase.

The $P(k)$ plot (not shown) of the $\{s(k)\}$ that has been obtained via Eq. (2b) and with $u=5$ ($f_r=M/T=2^4=W/2$, $N=2^{15}$) supports the prediction of our error analy-

sis. The $P(k)$ values are lowest in regions around $t=\pm 0.125$, where $s(t)$ is maximum [see Fig. 5(b)], and are largest in regions around $s(t)=0$.

It is also interesting to note that the performance of the SH technique (closed squares) keeps improving with increasing u since the ε plot decreases with u . The decrease continues until the sampling interval $\Delta=T/2M=2^{-u}$ becomes equal to δ itself, which happens at $u=20$.

To complete our study, we compare the performance of the recovery procedure with the results that are obtained from a q -bit AD converter that is used to sample $s(t)$ at the same value of Δ . For a q -bit (bipolar) AD converter, the quantization error E_{AD} is independent of the amplitude of $s(t)$ and it is given by $E_{AD}=2A/2^q$, where $\pm A$ are the power supply voltages.

Figure 6 presents the ε versus q plot of the q -bit AD converter for the case where $s(t)=\cos^{200}(2t-0.25)+\cos^{200}(2t+0.25)$, $A=\pm 2.5$, $T=1$, and $2M=32$. The ε value decreases exponentially with the bit number q of the AD converter. A comparison with Fig. 5(a) reveals that the application of the recovery method to SC's that are obtained with $2M=32$ and $N=2^{15}$ will yield results that are equivalent to those obtained using a 13-bit AD converter.

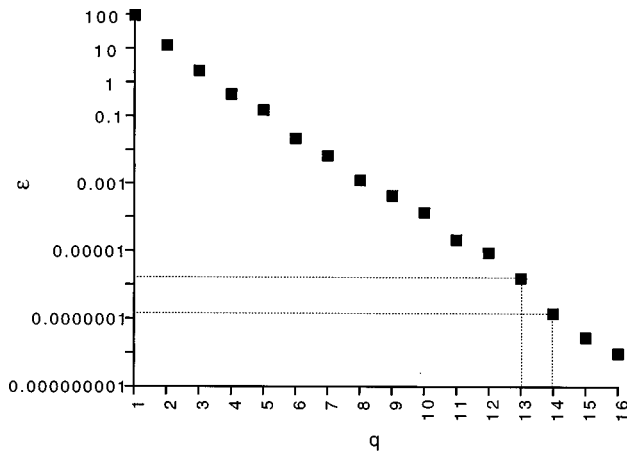


FIG. 6. NMSE vs q where q is the bit number of the AD converter. Test signal: $s(t) = \cos^{200}(2t - 0.25) + \cos^{200}(2t + 0.25)$, where $A = \pm 2.5$, $T = 1$, $2M = 32$, and $\Delta = 1/32$.

IV. COMPUTATIONAL COMPLEXITY

Besides reducing the processing time, less complexity is desired in a recovery algorithm to minimize the accumulation of the quantization errors into large rounding-off errors [17]. The spectral-based algorithm [1,2] previously used to calculate the $2M$ Fourier coefficients $\{c(m)\}$ from $\{t_i\}$, has a computational complexity of order $(2M)^2$. The recovery of $\{s(k)\}$ by inverse Fourier transforming $\{c(m)\}$ introduces an additional computational cost of $(2M)\ln(2M)$. Thus the total cost of recovering $\{s(k)\}$ from $\{t_i\}$ is $(2M)^2 + (2M)\ln(2M)$.

The cost of calculating $\{s(k)\}$ from $\{t_i\}$ via Eq. (2b) or Eq. (3), is of order $(2M)^3$ if done using the LU decomposition algorithm [20]. Cubic-spline interpolation on the other hand, has a complexity of order $(2M)$. The sample-and-hold (SH) method has a constant computational overhead cost due to the substitution that we perform into the reference function. Both the CS and SH methods, however, were found to be inferior against those that use either Eq. (2b) or Eq. (3).

Interpolation using higher-order spline (HOS) functions does not necessarily yield better results. The HOS interpolation normally needs a higher density of data points within the

region of concern. It also requires a higher degree of continuity. If the data points used are distant from the point of interest, the resulting higher-order polynomial tends to oscillate from the true value [20]. Adding more points close to the desired point usually helps, but this implies the use of finer sampling, which may not be available.

V. CONCLUSION

An approach has been presented for determining the equally sampled amplitude values $\{s(k)\}$ of $s(t)$ directly from its SC locations $\{t_i\}$. It is applicable to any band-limited continuous-time signal $s(t)$ with highest frequency $W/2$, that is, SC sampled using a reference frequency $f_r \geq W/2$, and a reference amplitude $A > |s(t)|$ for all t values.

The approach that makes use of the ideal interpolation formula is compared with other more common recovery methods. Numerical results indicate that the proposed method is reliable and practical to implement. The equally sampled value $s(k)$ is solved inversely from the convolution sum given in Eqs. (2b) or (3), and the accuracy of the result is affected by the quantization errors that exist in each of the sampling intervals Δ within the sampling period T .

The robustness of the calculated $s(k)$ values to rounding-off errors depends on the complexity of the inversion algorithm being used to solve Eq. (2b) or (3). Thus, a worthwhile goal is to find an algorithm for implementing Eq. (2b) or (3), which is less complex than the current one, which is of order $(2M)^3$.

More efficient computation of $\{s(k)\}$ can be also achieved if the correct inverse relation to Eq. (2b) or (3) could be found that expresses the $s(k)$ value as a (convolution) sum of the $2M$ $r(t_i)$ values. Even the direct solution of such an inverse relation would involve a computational complexity that is of order $(2M)^2$.

ACKNOWLEDGMENTS

The authors are grateful to Marisciel Litong for her help with the numerical experiments. This work is partially supported by the Office of Research Coordination, University of the Philippines.

-
- [1] C. Blanca, V. Daria, and C. Saloma, *Appl. Opt.* **35**, 6417 (1996).
 [2] C. Saloma and P. Haeberli, *Appl. Opt.* **32**, 3092 (1993).
 [3] V. Daria and C. Saloma, *Rev. Sci. Instrum.* **68**, 240 (1997).
 [4] J. Proakis and D. Manolakis, *Digital Signal Processing: Principles, Algorithms, and Applications*, 2nd ed. (Macmillan, New York, 1992).
 [5] S. Rice, in *Selected Papers on Noise and Stochastic Processes*, edited by N. Wax (Dover Publications, New York, 1954) p. 133.
 [6] C. Koch, *Nature (London)* **385**, 207 (1997).
 [7] D. Fitzpatrick, R. Batra, T. Stanford, and S. Kuwada, *Nature (London)* **388**, 871 (1997).
 [8] J. Hopfield, *Nature (London)* **376**, 33 (1995).
 [9] E. Bagarinao and C. Saloma, *Phys. Rev. E* **53**, 5516 (1996).
 [10] G. Deco and B. Schürmann, *Phys. Rev. Lett.* **79**, 4697 (1997).
 [11] D. Ferster and N. Spruston, *Science* **270**, 756 (1995).
 [12] T. Bullock, *Rev. Neurosci.* **16**, 1 (1993); J. O'Keefe and M. Recce, *Hippocampus* **3**, 317 (1993).
 [13] W. Heiligenberg, *Neural Nets in Electric Fish* (MIT Press, Cambridge, MA, 1991).
 [14] A. V. M. Herz and J. J. Hopfield, *Phys. Rev. Lett.* **75**, 1222 (1995).
 [15] S. Levin, B. Grenfell, A. Hastings, and A. Perelson, *Science* **275**, 334 (1997).
 [16] Y. Zeevi, A. Gavriely, and S. Shamai, *J. Opt. Soc. Am. A* **4**, 2045 (1987); A. Requicha, *Proc. IEEE* **68**, 308 (1980).
 [17] C. Saloma, *J. Appl. Phys.* **74**, 5314 (1993).
 [18] J. Gaskill, *Linear Systems, Fourier Transforms, and Optics* (Wiley, New York, 1978), pp. 223–285.

- [19] D. Manolakis and J. Proakis, *Introduction to Digital Signal Processing* (Maxwell-Macmillian, New York, 1988).
- [20] W. Press, W. Vetterling, S. Teukolsky, and B. Flannery, *Numerical Recipes in C*, 2nd ed. (Macmillan, New York, 1992), pp. 32–55, 115, 500–503.
- [21] L. Yaroslavsky, *Appl. Opt.* **36**, 460 (1997).
- [22] Equation (3) is derived from Ref. [21] [Eq. (2)], where $M = N$ (Ref. [21] notation). To be consistent with our overall notation, the upper limit was changed from N to $2M$, and the sampling interval from Δx to Δ . Since we are interested in the amplitude values at the middle of each sampling interval, we placed an offset of $1/2$ on index n , i.e., $(n - 1/2) = (2n - 1)/2$. Note that for SC sampling $\Delta = 1/2 f_c$.
- [23] All computations were performed in a DEC AlphaServer 2000 4/275 running Digital Unix 3.2D (Six-digit decimal precision, Floating-point range: $1.401\ 298\ 464\ 324\ 817\ 07 \times 10^{-45}$ – $3.402\ 823\ 466\ 385\ 288\ 60 \times 10^{38}$). All numerical codes were done in *C* and compiled using the DEC *C* compiler.